Supporting Information for

A controlled nucleation and growth of Si nanowires by using TiN diffusion barrier layer for lithium ion batteries

*Dongheun Kim[1], Towfiq Ahmed[2], Kenneth Crossley[1], J. Kevin Baldwin[1], Sun Hae Ra Shin[1, §], Yeonhoo Kim[1], Chris Sheehan[1], Nan Li[1], Doug V. Pete[4], Henry H. Han[1, §, *], Jinkyoung Yoo[1, *]*

[1]Center for Integrated Nanotechnologies, Los Alamos National Laboratory, Los Alamos, NM 87545, United States of America

[2]T-4, Los Alamos National Laboratory, Los Alamos, NM 87545, United States of America

[4]Center for Integrated Nanotechnologies, Sandia National Laboratories, Albuquerque, NM 87110, United States of America

[§]Present address : Pacific Northwest National Laboratory, Richland, WA, 99354, United States of America

Density functional theory calculation: All calculations are performed using the planewave pseudo-potential code VASP[1–3] under the generalized gradient approximation of Perdew, Burke, and Ernzerhof (PBE)[4]. For atomic core-levels, we have used projected augmented wave (PAW) potentials[5,6] treating the 2s2p of N, 4s4d of Ti, 6s5d of Au, and 3s3p of Si as the explicit valence electrons. For all calculations, the total energy during electronic relaxation is converged to 10^{-6} eV while the force/atom during ionic relaxation is converged to 0.01eV/°A. A maximum energy cutoff of 400 eV is used for plane-wave basis set. Our TiN slab/vacuum system has 4 layers of Ti-N planes (Fig.S1-b) in the 100 direction with a unit cell with a = b = 6.22 Å, c = 16.6 Å, and $\alpha = \beta = \gamma = 90^{o}$. There are 16 N and 16 Ti atoms in this supercell. Similarly, our Si

slab/vacuum system has 3 layers of Si hexagonal lattice (Fig.S1-d) in the 111 direction with 24 Si atoms in the unit cell with a = b = 7.68 Å, c = 17.05 Å, $\alpha = \beta = 90^{o}$, and $\gamma = 120^{o}$. To incorporate the vdW interaction, we have used optB86bvdW functional where the exchange functionals were optimized for the correlation part [7]. Therefore, the LDA correlation
part present in the PBE functional is removed by using the parameter AGGAC = 0.000 in the input file in order to avoid double-counting. For ionic relaxations, we have used Γ point to sample the Brillouin zone. To find the transition states (reaction path) between the initial (unclustered) and final (clustered) states, we used Nudged Elastic Band (NEB) [8] method implemented in VASP code. This method find the minimum energy path and saddle points between the reactant (initial) and product (final) states. The reaction path provides diffusion barrier which indicates kinematical likelihood of a transition from initial to final state. In our case, the transition will be from an unclustered to a clustered (agglomerated) state of Au atoms on TiN and Si surface. Also for comparison, we performed calculation for Au clustering on Fe(111) surface with 36 Fe atoms in the unit cell.

To study the agglomeration (on Si) or array formation (on TiN) of Au atoms, we considered 4 Au atoms on TiN(100) surface and 3 Au atoms on Si (111) surface. Our calculations are performed in two major steps. First, we identified the most energetically preferred adsorption location of a single Au atom on Si and TiN surface. As shown on Fig. S1(b), the most energetically preferred and possible symmetric points on TiN (100) surface are located at (i) center of square (A1), top of Ti atom (A2), and top of N atom (A3). By doing a full ionic relaxation of the Au atom as well as the top two layers of TiN (while keeping the bottom two layers fixed), we found the most energetically stable location is A1. On Si(111) surface, we observe a top honeycomb hexagonal layer which is be further split into two sub-layers of triangular lattices. The three most energetically stable points are the central of the hexagon (B1), top of the bottom layered Si (B2), and top of the top layered Si (B3) (Fig. S1(d)). After full ionic relaxation of a single Au atom on Si (111) surface, we found the Au atom on top of the hexagon center (B1) has the lowest energy (most stable) configuration.

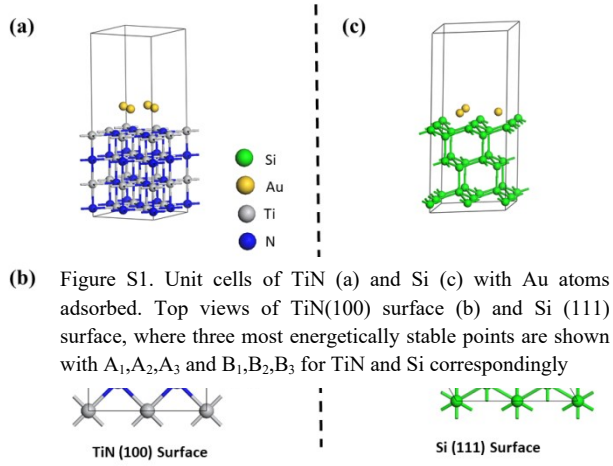

Figure S1. Unit cells of TiN (a) and Si (c) with Au atoms adsorbed. Top views of TiN(100) surface (b) and Si (111) surface, where three most energetically stable points are shown with A_1,A_2,A_3 and B_1,B_2,B_3 for TiN and Si correspondingly

In the second step, we used the most stable locations (A1 and B1) on TiN and Si surfaces, and calculated the transition path for Au atoms cluster formation. The *initial state* is a geometrically optimized structure which has 3 neighboring Au atoms on A1 locations, and the fourth atom is located on the next nearest A1 site. In the final state, another geometry optimized structure is prepared where all four Au atoms are clustered on the nearest neighboring points, where the system is geometry optimized. In between the initial and final states, the minimum energy path with four more transition states is calculated using Nudged-Elastic bands (NEB) method.

Cyclic Voltammetry: Cyclic voltammetry was performed on Si(P) nanowires (NWs) grown directly on titanium nitride (TiN) on stainless steel (SS) and plain SS substrates after 500 galvanostatic charge/discharge cycles (at approximately 0.2 C). The scan rate was 0.1 mV/s and the potential range was 1.5 V to 10 mV vs Li/Li^+. The NWs on SS displayed lithiation peaks around 200 mV and 25 mV, while the NWs on TiN displayed lithiation peaks around 175 mV and 12 mV. Both growth conditions displayed delithiation peaks around 340 mV and 510 mV. These values are consistent with the two-step lithiation/delithiation of amorphous silicon discussed in the literature [9-11]. Overall, the data shown in Figure S2 clearly indicate that TiN does not react reversibly with lithium within the cell's working potential range, and thus does not contribute to the increased retained capacity observed for Si(P) NWs grown on TiN.

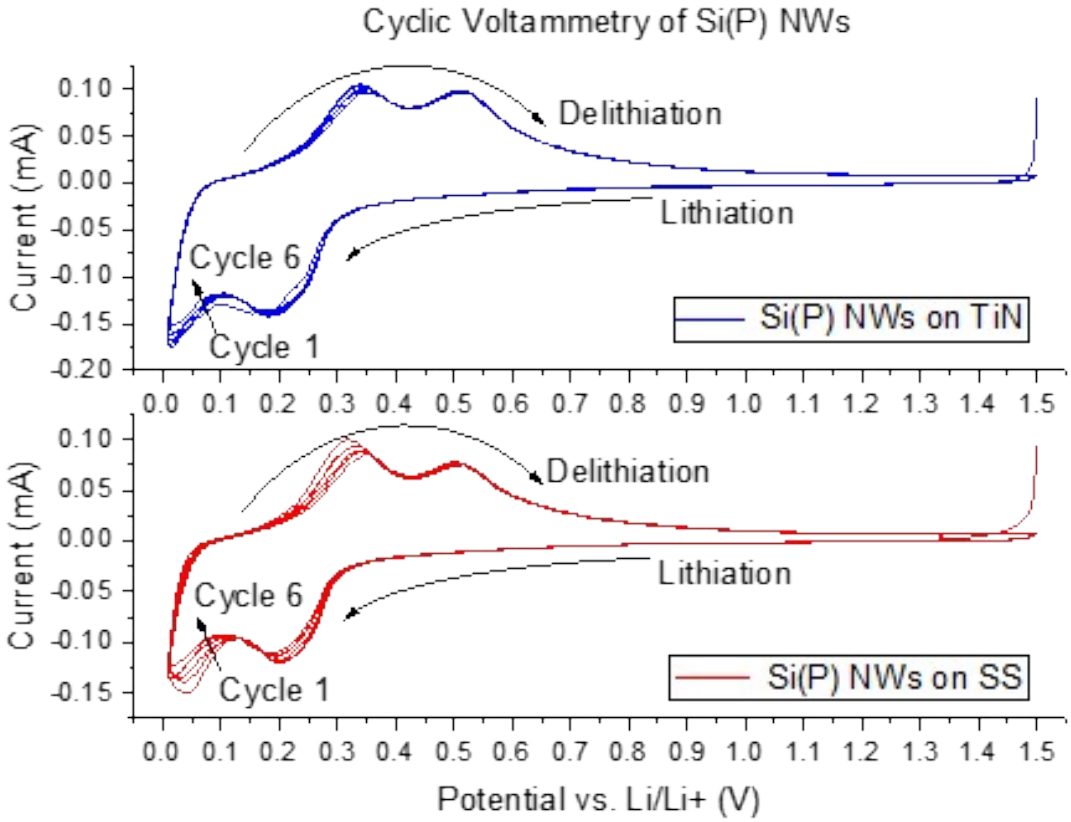

Figure S2. Cyclic voltammetry of Si(P) NWs on TiN (blue) and SS (red) after 500 cycles.

References:

[1] Kresse, G; Furthmuller, J. *Phys. Rev. B* **1996**, 54, 11169.

[2] Kresse, G.; Hafner, J. *Phys. Rev. B* **1993**, 47, 558.

[3] Kresse. G; Furthmller, J. *Comput. Mater. Sci.* **1996**, 6, 15.

[4] Perdew, J. P.; Burke, K.; Ernzerhof, M. *Phys. Rev. Lett.* **1996**, 77, 3865.

[5] Vanderbilt, D. *Phys. Rev. B* **1990**, 41, 7892.

[6] Kresse G.; Hafner, J. *J. Phys.: Condens. Matter.* **1994**, 6, 8245.

[7] Klimeš, J.; Bowler, D. R.; Michaelides, A. *Phys. Rev. B* **2011**, 83,195131.

[8] Henkelman G.; Jonsson. H. *J. Chem. Phys.* **2000**, 113, 9901.

[9] Chan, C. K, et al. *Nature Nanotech* **2008**, *3* (1), 31–35.

[10] Kang, K, et al. *Appl. Phys. Lett.* **2010**, *96* (5), 053110.

[11] Obrovac, M. N.; Krause, L. J. *J. Electrochem. Soc.* **2006**, *154* (2), A103.